Title

ANGLE-RESOLVED PHOTOEMISSION FROM VALENCE BANDS OF Cu AND Au SINGLE CRYSTALS USING 32 - 200 eV SYNCHROTRON RADIATION

Author

Stohr, J.

Publication Date

1976-06-01

Submitted to Physical Review B

LBL-5149
Preprint C.1

ANGLE-RESOLVED PHOTOEMISSION FROM VALENCE BANDS OF Cu AND Au SINGLE CRYSTALS USING 32 - 200 eV SYNCHROTRON RADIATION

J. Stöhr, G. Apai, P. S. Wehner, F. R. McFeely,
R. S. Williams, and D. A. Shirley

June 1976

Prepared for the U. S. Energy Research and
Development Administration under Contract W-7405-ENG-48

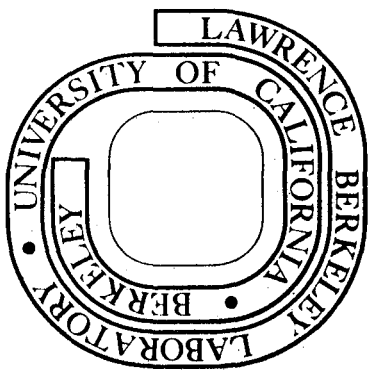

DISCLAIMER

LBL-5149

ANGLE-RESOLVED PHOTOEMISSION FROM VALENCE BANDS OF Cu AND Au SINGLE CRYSTALS USING 32 - 200 eV SYNCHROTRON RADIATION*

J. Stöhr, G. Apai, P. S. Wehner, F. R. McFeely,
R. S. Williams, and D. A. Shirley

Materials and Molecular Research Division
Lawrence Berkeley Laboratory
and
Department of Chemistry
University of California
Berkeley, California 94720

June 1976

ABSTRACT

The directional anisotropy in photoemission from valence bands of Cu and Au single crystals has been studied in the photon energy ranges 32 eV $\leq h\nu \leq$ 200 eV, and 32 eV $\leq h\nu \leq$ 130 eV, respectively. Angle resolved photoemission energy distributions (PED's) were obtained for electrons emitted in the [001] and [111] directions. Dramatic differences were found between the two directions and strong variations with energy were obtained over the entire energy range. The results are discussed in terms of final-state band structure effects and/versus strong inelastic damping in the final state. For Cu, spectra taken at $h\nu$ = 90 eV along the same symmetry directions at high (90°) and low (35°) take-off angles from the surface show a pronounced narrowing of the d-band at low take-off angles. This is attributed to a preferential sampling of the local density of states at the surface by using an appropriate photon energy and take-off angle. The energy dependence

of the Au 5d intensity has been measured and is found to decrease by a factor of $\sim$50 over the investigated photon energy range 40 - 190 eV.

I. INTRODUCTION

Angle resolved photoemission (ARP) from single crystals has previously been reported in the ultraviolet (UPS)[1] and x-ray (XPS)[2,3] photoemission ranges. In the two regimes significantly different information is contained in the experimentally observed photoelectron energy distributions (PED's). At UPS energies the PED's obtained by exciting valence electrons are determined by the details of both the initial (valence band) and final (conduction band) state energies and wavefunctions.[4,5] In this regime the three step model of photoemission[5] including strict momentum and energy conservation during the excitation process, has proven to describe the experimental situation quite well. On the other hand, angle resolved PED's observed at XPS energies basically depend only on the symmetry properties of the initial states.[3] In this case momentum- and energy-conservation selection rules are also important but they are more easily satisfied. Thus final-state band structure effects are weak. The experimental spectra are well described by the initial density of states modulated by an angle dependent matrix element.[3]

So far, no ARP studies have been performed in the transition region between UPS and XPS, namely in the region 40 eV $\lesssim h\nu \lesssim$ 1000 eV. Here we report such experiments. We have utilized the first six 8-hour shifts dedicated to synchrotron radiation on the SPEAR storage ring at the Stanford Synchrotron Radiation Project (SSRP).[6] The high photon flux emitted by SPEAR, which operated at beam currents up to 80 mA,[7] allowed ARP studies of the valence bands (VB) of Cu (3d) and Au (5d) single crystals in the energy range up to 280 eV for Cu and 130 eV for Au.

ARP experiments in the photon energy range studied here are of considerable interest because of their high surface sensitivity which arises from a minimum in the photoelectron mean free path in the kinetic energy region around 100 eV.[8] In this range of electron energies the mean free path becomes comparable with the interatomic distance in the solid, and the photocurrent arises largely from the top layers.[1] The theoretical description of the PED's in this range of "strong damping" is a difficult problem. Not only does one have to consider the local states of the outermost surface layer in addition to the bulk states as possible initial states, but the photoemission process per se can no longer be described by a simple model because the steps of excitation, transport, and emission are inextricably mixed.[9] It has been argued that because of strong inelastic electron scattering effects the observed spectra might even have to be interpretated in terms of many body effects rather than single particle properties like densities of states.[1]

This paper is intended to elucidate some of the above problems by providing the first experimental ARP results in this interesting energy range. It is apparent that ARP studies provide considerably more detailed information than the previously available angle integrated results.[5,10,11,12] Experimental details and results are presented in Sections II and III, respectively. In Section IV we discuss the basic physical reasons for an energy and angular dependence of photoemission in the UPS-XPS transition region. The experimental results for Cu and Au are discussed in these terms in Section V. In the concluding Section VI we discuss the basic information obtained from the present investigation and point out some of the problems stimulated by it.

II. EXPERIMENTS

The experimental geometry is shown in Fig. 1. The monochromatic[13] photon beam was incident on a Cu or Au single crystal which was positioned at the focal point of a cylindrical mirror analyzer (CMA) modified for ARP studies as discussed below. The electric field vector $\vec{E}$ of the incident radiation lay in the plane defined by the beam and the propagation direction of electrons accepted by the analyzer. Its orientation with respect to the crystalline axes is shown in Fig. 2. We have chosen the fourfold cubic axes [100], [010], and [001] as our frame of reference (x,y,z) and we describe the spacial orientation of the $\vec{E}$ vector and the detector in terms of polar (Θ) and azimuthal (ϕ) angles. The positions of the x-ray beam and the detector were fixed relative to each other with the x-ray Poynting vector, $\vec{E}$ vector, and the detector acceptance axis lying in the horizontal plane.

The sample holder could be rotated about a vertical axis. Two crystals with a (001) and (111) face, respectively, were mounted simultaneously on the sample holder. By raising or lowering the sample holder the electrons were collected either along the [001] direction of the (001) crystal or along the [111] direction of the (111) crystal (cp. Fig. 2). For Cu it was possible to look at photoelectrons emitted along both the [001] and [111] axes of the same crystal by rotating about the vertical axis. The faces of the crystals were polished to 1 micron smoothness and then etched before introduction into the ultra-high vacuum ($\sim 1 \times 10^{-10}$ Torr) chamber. The surfaces were then cleaned by argon ion bombardment and annealed by heating with an electron gun to remove surface damage.

The CMA, operated in the retarding mode,[14] was adapted for angle-resolved measurements by placing a stainless-steel shield with a 11° slit aperture on the front of the analyzer.[15] The geometrical arrangement of the slit is shown in Fig. 1b. The modified analyzer accepts electrons emitted into a cone of approximately ±6°. The effective acceptance area of the CMA is defined by the ±6° acceptance width of the CMA[16] and by the ±5.5° slit width of the shield (cp. Fig. 1b). It was found that the shield reduces the counting efficiency of the CMA by approximately 360°/11°, as expected. The Cu PED's were recorded at a pass energy (E_p) of 10 eV, except for the $\hbar\omega$ = 200 eV spectra which were measured with E_p = 15 eV for Cu [001] and E_p = 25 eV for Cu [111]. The Au spectra were obtained with E_p = 50 eV. At a given pass energy the CMA used in the present study had an energy resolution of $\Delta E = 0.016\ E_p$ when operated without the slit aperture. It was found that the slit aperture improves the energy resolution of the analyzer. Measurements of core levels with and without the slit aperature showed that the resolution improves by approximately a factor of 2 when the aperture was used.[17] We thus believe that the Cu and Au spectra were recorded with a CMA resolution of $\Delta E < 0.15$ eV and $\Delta E \approx 0.4$, respectively.

The angle-resolved experiments presented here were carried out in the photon energy range 32 eV $\leq h\nu \leq$ 200 eV for Cu and 32 eV $\leq h\nu \leq$ 130 eV for Au. The lower experimental limit (32 eV) is given by the possible mechanical motions of the monochromator.[13] The upper limit for Cu is given by the resolution[18] of the monochromator. We recorded Cu spectra up to $h\nu$ = 280 eV (for even higher energies the absorption of carbon (K-edge) on the various mirror surfaces resulted in a

considerable decrease in intensity), but above $h\nu \approx 200$ eV the resolution decreased considerably and no difference in the PED's for Cu [001] and Cu [111] could be observed.[18] The upper limit ($h\nu = 130$ eV) for Au was determined by the small Au 5d cross section at higher energies as will be discussed in more detail below. The low 5d cross section was also the reason for recording the Au PED's at a higher CMA pass energy.

In order to obtain information on the cross-section variation of the 5d band in Au with photon energy we have measured the variation of the 5d intensity in the range 40 eV $\leq h\nu \leq$ 190 eV. These studies were carried out with a resolution $\Delta E = 1.6$ eV ($E_p = 100$ eV). No aperture was used in order to average over various angles of electron emission and in order to improve the signal. The Au sample was a polycrystalline foil which was cleaned by argon ion bombardment and subsequently annealed by heating with an electron gun to remove surface damage.

III. RESULTS

A. Cu

Experimental results for Cu are shown in Fig. 3. For both crystal faces the electrons were taken off along the surface normals of the (001) and (111) faces as shown in Fig. 2. The experimental orientations are summarized in Table I. The spectra are shown expanded around the Fermi energy, because the onset of photoemission is often very weak for Cu.

Several distinct trends are apparent in the PED's shown in Fig. 3. The 4s band, between the Fermi energy and 2 eV binding energy (BE), is strongest in the range 70 - 120 eV for Cu [001] and 60 - 85 eV for

Cu [111]. Its strength, relative to the d-band intensity, is larger for Cu [111] than for Cu [001]. In Fig. 4 some PED's observed along the [001] and [111] directions are compared with each other. For all photon energies distinct differences are observed. Note that we have included some spectra ($h\nu$ = 80,90,110 eV) in Fig. 4 which are not shown in Fig. 3. The d-band extends from $\sim$2 eV to $\sim$6 eV BE. For Cu [001], the most striking changes occur in the range 70 eV $\leq \hbar\omega \leq$ 130 eV. A feature at $\sim$5 eV BE shows a broad resonance in intensity, peaking near $\hbar\omega$ = 110 eV (compare Figs. 3 and 4). The PED's for Cu [111] exhibit a similar resonance in intensity of a peak at $\sim$5 eV BE in the range 60 $\leq \hbar\omega \leq$ 100 eV, with a maximum at $\hbar\omega \approx$ 80 eV (compare Figs. 3 and 4). At the highest photon energy (200 eV) this feature appears again to increase in intensity.

Fig. 5 demonstrates the sensitivity of the PED's to the experimental geometry at $h\nu$ = 120 eV. The dashed line correspond to a spectrum taken at normal take-off from the (001) face and is identical to the Cu [001] spectrum at $\hbar\omega$ = 120 eV in Fig. 3. As seen from Table I or Fig. 2a this geometry corresponds to an angle Θ = 27.5° between the $\vec{E}$ vector and the fourfold z axis. The PED shown as a dashed curve in Fig. 5 was obtained by merely rotating the (001) crystal by 4° about a vertical axis such that in this case Θ = 23.5° (compared Fig. 2a). The difference between the two spectra in Fig. 5 is quite striking and it represents the strongest angular variation observed in the studied photon energy range.

In Fig. 6 we compare PED's taken at $h\nu$ = 90 eV along a special symmetry direction ([001] or [111]) from different crystal faces.

Electrons were taken off along the [001] direction either normal to the (001) face ($\alpha = 90°$) or at a take-off angle $\alpha \approx 35°$ with respect to the (111) face (compare Fig. 2). In the latter case the sample holder was rotated by $\sim 55°$ about a vertical axis and raised to place the (111) crystal instead of the (001) crystal in the focal point of the x-ray beam and analyzer. Similarly, PED's were obtained for propagation along the [111] direction of the (111) crystal ($\alpha = 90°$) and the (001) crystal ($\alpha = 35°$). As seen from Fig. 6 there are distinct differences between the corresponding PED's of electron propagation. In both cases the spectra obtained at low take-off angles ($\alpha = 35°$) exhibit a narrowing in d-band width and increase in height at their center of gravity.

B. Au

PED's measured along the [001] and [111] directions from Au single crystals are shown in Fig. 7. The electrons were collected normal to the (001) and (111) faces, respectively. The experimental situation is shown in Fig. 2 and summarized in Table I. For both orientations the s-band extending from the Fermi level to about 2 eV BE is most pronounced in the energy range 30 - 80 eV and loses intensity relative to the d-band peaks above 80 eV. The d-band for Au consists of two main peaks centered around 3.5 eV and 6.5 eV BE. Both peaks can be approximately described as being composed of two components at ~ 3 eV and ~ 4 eV and ~ 6 eV and ~ 7 eV BE, respectively. The energy dependence of the PED's for both directions essentially consists of intensity changes of these

four peaks. Spectra for electron emission into the [001] and [111] directions are compared in Fig. 8. As for the case of Cu, distinct changes between the two directions are observed.

The energy dependence of the Au 5d VB intensity in the range $40\ eV \leq h\nu \leq 190\ eV$ is shown in Fig. 9 as a solid line. For comparison we have also included the Ag 4d VB photoemission intensity variation[12] in the figure. While the d-band intensity is given in arbitrary units, we have normalized the Ag 4d and Au 5d intensities to each other experimentally by comparing the areas under the PED's from Ag and Au at $h\nu = 40\ eV$. The data points for Au shown in Fig. 9 were obtained by correcting the Au spectra for their inelastic background, measuring the area under the PED's in the binding energy range $2\ eV \leq h\nu \leq 8\ eV$, and correcting this area with respect to the incident photon flux and the collecting efficiency of the CMA.[12]

IV. GENERAL DISCUSSION OF ARP IN THE UPS - XPS TRANSITION REGION

In general, photoemission spectra depend on by the details of the initial (valence band) and final (conduction band) state energies and wavefunctions. Analysis of experimental PED's thus requires the knowledge of these quantities. In the ultraviolet range ($h\nu \leq 40\ eV$) photoemission spectra are usually analyzed by comparison with existing band structure calculations assuming strict momentum and energy conservation in the excitation process. For example, ARP studies of Cu[19] and Au[20] at photon energies 16.8 eV and 21.2 eV were discussed in terms of the band structure calculations by Janak et al.[21] and Christensen and

Seraphin.[22] The interpretation of ARP spectra in the x-ray regime ($h\nu \geq 1000$ eV) is simplified by the fact that the details of the final state band structure are unimportant. In this case the PED's are determined by the symmetry properties of the initial states alone.[3] In the photon energy range covered in the present study, final-state and transition-matrix-element effects are expected to be important. Because band structure calculations are usually available[23] only to about 40 eV above the Fermi level the description of the final state is thus a major problem.

In a previous paper on polycrystalline Cu[11] we used a free electron band structure and orthogonalized-plane-wave wavefunctions to describe the final state. However, in contrast to angle integrated photoemission from polycrystalline samples, angle resolved spectra from single crystals are far more sensitive to the exact nature of the final-state Bloch function. In a bulk interband optical transition an electron is ejected whose wavefunction

$$\Psi_f(\vec{r}) = \sum_{\vec{G}} a_{\vec{G}} \exp[i(\vec{k} + \vec{G}) \cdot \vec{r}] \qquad (1)$$

has plane-wave components going in different directions $\vec{k} + \vec{G}$, where $\vec{G}$ is a reciprocal lattice vector.[24] The intensity of emission into the directions $\vec{k} + \vec{G}$ is determined by the respective coefficients $a_{\vec{G}}$ in equation (1). By assuming free electron final states all but the leading term in equation (1) are omitted and the electron may only leave in one direction. The resulting overemphasized angular anisotropies in the free electron final state picture are somewhat averaged out in angle-integrated photoemission[11] but preclude predicting the PED's observed

in angle resolved studies.

In the intermediate photon energy range studied here another problem arises in the description of the final state. Because of strong inelastic scattering[8] the final state wavefunction no longer represents a pure Bloch-wave characteristic of the bulk, but must include damping due to inelastic effects inside the solid. This may be accounted for in an ad hoc fashion by replacing the (surface) normal component of the wavevector in the final-state wavefunction by a complex quantity, which will exponentially favor emission from the surface layers.[25] The imaginary part then describes damping of the electron wavefunction inside the solid and may be related to the familiar mean free path.[26] In principle, with this ad hoc modification of the final state wavefunction, the ARP spectra presented here could be analyzed by using a band-structure calculation which extends to higher energies. However, we feel that a more appropriate approach may be to calculate the photoemission spectra by using the multiple-scattering formalism[27] employed in current low-energy electron diffraction (LEED) theories.[28] Within this formalism inelastic effects may be included by inserting a complex optical potential into the single particle propagator.[29] Within the framework of the present paper no such calculation is attempted, but instead we discuss ARP in the UPS - XPS transition region in general terms and restrict the analysis of our experimental results to some basic observations.

At the intermediate photon energies used in the present study the changes in the PED's with emission direction are in part determined by the wavevector dependence of the final state energies and wavefunctions.

For photoemission along the [001] and [111] directions only final Bloch states which contain coefficients (cp. equation (1)) $a_{[oon]}$ (n = 0,2,4,6...) and $a_{[mmm]}$ (m = 0,1,3,5...), respectively, can contribute in a bulk photoemission process. This selection of final states is a consequence of momentum conservation. Even in the region of highest surface sensitivity, i.e. maximum broadening of the normal component of the photoelectron wavevector, the parallel wavevector components are conserved. However, momentum broadening in the final state will weaken final state effects. Because of momentum conservation selection rules the nature of the final state also determines which initial states in the first Brillouin Zone (BZ) are sampled. For photoemission along a given symmetry line only states in the first BZ along this line contribute.[30] The finite acceptance angle of the photoelectron analyzer results in sampling all initial states whose $\vec{k}$ vectors lie within a cone centered around the symmetry direction. The cone diameter depends on the photon energy, as discussed below.

The observed modulation effects in the PED's with photon energy arise mainly because of excitation into different final-state regions. In general, both the number of final states that satisfy energy and momentum conservation and the final-state Bloch functions (which determine the transition matrix element)[31] will change with photon energy. The number of final states increases with increasing photon energy and the leading coefficients in the Bloch functions (equation (1)) will correspond to larger reciprocal lattice vectors. For example, at $h\nu$ = 50 eV photoemission along the [001] direction is strongly determined by the $a_{[002]}$ component of the final state Bloch function

(equation (1)), while the $a_{[004]}$ component is most important at $h\nu$ = 150 eV.[32] The magnitude of the reciprocal lattice vector involved in the umklapp process of the final state wavevector into the first BZ also determines how large a fraction of the first BZ (initial states) contributes to the ARP process. This is illustrated in Fig. 10b for photoemission into the [001] direction. We have assumed a ±6° acceptance angle of the analyzer (dashed area), which is superimposed on the (010) projection of the three dimensional BZ of the fcc lattice (compare Fig. 10a). Depending on the photon energy the final state will lie in either the first, second, third, etc. BZ and either the $\vec{G}$ = [000], $\vec{G}$ = [002], $\vec{G}$ = [004], etc. reciprocal lattice vector will characterize the final state. The dashed area in the respective BZ in Fig. 10b is then exactly the part of the zone which may be sampled in the first BZ (initial states) by means of an umklapp process involving the corresponding $\vec{G}$ vector.

It is interesting to discuss what happens at high photon energies; i.e., at XPS energies ($h\nu \gtrsim 1000$ eV). Here the number of final states is large and a sufficient number of Bloch waves contain an appropriate reciprocal lattice vector which reflects the final state back into the first BZ by means of an umklapp process. Because of the magnitude of these vectors involved the whole first BZ is sampled. The PED's are then determined by the transition matrix element between the initial states and the appropriate plane-wave components of the final states (equation (1)). As has been shown in an earlier paper[3] photoemission along the [001] and [111] directions samples the e_g and t_{2g} projections of the initial density of states, respectively. After these general

considerations, we shall now be more specific and discuss some features of the measured PED's for Cu and Au below.

V. DISCUSSION OF RESULTS

A. Cu

In contrast to the PED's from polycrystalline Cu samples which did not show any significant changes in spectral change above $h\nu \approx 80$ eV,[11] the spectra in Fig. 3 have not yet converged to a constant shape even at $h\nu = 200$ eV. Note in particular the opposite changes in width of the d-band for Cu [001] and Cu [111] in the range $130 \text{ eV} \leq h\nu \leq 200 \text{ eV}$. These changes with photon energy are thought to arise mainly from direct transitions. The dramatic intensity modulation of the two d-band peaks at $h\nu = 120$ eV (Fig. 5) which was obtained by changing the emission direction only 4°, also indicates the importance of direct transitions at photon energies above 100 eV. It is somewhat surprising that the energy dependence of the PED's is quite weak at the lowest energies studied ($h\nu \leq 60$ eV). We have taken additional spectra in the range $32 \text{ eV} \leq h\nu \leq 40 \text{ eV}$, in increments of 2 eV, which showed a smooth trend from the spectral shape at 32 eV to that at 40 eV shown in Fig. 3.

The region $70 \text{ eV} \leq h\nu \leq 100$ eV is particularly interesting, as the PED's for Cu [001] and Cu [111] bear a close resemblence to the e_g and t_{2g} projections of the Cu 3d valence band. We have calculated the total density of states and its e_g and t_{2g} projections using Smith's[33] parameterization of the Hodges, Ehrenreich, and Lang[34] tight binding interpolation scheme. The results are shown in Fig. 11. For Cu, a pronounced difference exists between the e_g and t_{2g} projections, and ARP measurements at XPS energies[35] for Cu [001] and Cu [111] indeed

show the spectral shapes predicted by the above calculation. The question arises why the d-band features around 85 eV resemble the XPS results. From our previous results on polycrystalline Cu[11] and also from recent work on Au,[36] there appears to be strong evidence that the minimum in escape depth for the noble metals Cu and Au occurs around 90 eV. At first sight the resulting momentum broadening in the final state, which weakens final state band structure effects, appears to be a good candidate to explain the observed PED's in the range around 85 eV. Let us discuss this possibility in more detail.

At XPS energies the PED's obtained along the [001] and [111] directions resemble the e_g and t_{2g} projections of the valance band for two basic reasons: 1) all initial states within the first BZ are sampled; 2) the transition matrix element can be interpreted using plane wave final states.[3] At $h\nu$ = 85 eV photoemission from the bulk, for example along the [001] direction, involves final states with $\vec{G}$ vectors of the form [00n] with the n = 2 and n = 4 components dominating. In this case photoemission into the $\Delta\Omega = \pm 6°$ acceptance cone of the analyzer dominantly derives from initial states within the first BZ which correspond to the dashed area in the second ($\vec{G}$ = [002]) and third ($\vec{G}$ = [004]) zone in Fig. 10b.[37] As is seen from Fig. 10b, all initial states which may contribute lie inside a cone centered along the k_z axis. At $h\nu$ = 85 eV and $\Delta\Omega = \pm 6°$ only part of the three-dimensional first BZ is sampled. If the inelastic mean free path is small, the normal component of the final-state momentum vector becomes ill-defined bacause of a loss of (infinite) lattice periodicity near the surface in the normal direction. The problem of sampling the

first BZ reduces to two dimensions (the $k_x - k_y$ plane). However, the area sampled in the $k_x - k_y$ plane does not increase by introducing momentum broadening in the k_z direction. Thus, although a relatively larger fraction of the first BZ is sampled in the momentum broadening case, an acceptance angle of ±6° does not appear to be sufficient at $h\nu$ = 85 eV to provide access to the whole two-dimensional BZ. Even if we assume for the sake of argument that the most important parts of the first BZ are being sampled, the plane-wave description of the final state at such low photon energies still needs to be justified. On the basis of atomic considerations one would in general expect the interaction between the photoemitted electron and the ion-core potential to lead to more complicated (energy dependent) angular distributions than those predicted by a plane wave final state. For photoemission from d-orbitals the angular distribution of the electrons is determined by the p and f partial-wave final-state channels. One important quantity which is a good indication of the strength of the interaction of the photoelectron and the ion-core, and hence of the validity of the plane-wave final-state description, is the phase shift.[38] Although we do not claim that the plane-wave final state description is valid for Cu at $h\nu$ = 85 eV, we note that phase shifts for Cu are considerably smaller than for Au.[39] For this reason one would not expect to see the same energy and angular dependences for the Cu and Au PED's in the surface-sensitive region. The Cu spectra around 85 eV might resemble the t_{2g} and e_g projections because both criteria 1) and 2) mentioned above are approximately satisfied.

One interesting question that arises in the intermediate photon energy regime concerns the effects of surface versus bulk photoemission.

In general, surface sensitivity may be achieved if either the initial or final state wavefunction is strongly localized at the surface. Such a situation is encountered for states at the surface whose energy corresponds to a band gap in the bulk.[1] Several studies in the ultraviolet regime of photoemission were concerned with the study of such surface states at clean metal surfaces.[40] For Cu, the existence of surface states has been postulated on experimental grounds by Gartland and Slagsvolt.[41] A peak at 0.4 eV below the Fermi level occuring in the PED's from Cu (111) at $h\nu \leq 6.6$ eV was interpreted as a surface band within the s-p band gap. A similar structure was also observed by Ilver and Nilsson[19] at $h\nu = 16.8$ eV. However, these authors pointed out an alternative explanation in terms of intraband excitations by the longitudinal electric field.[42] Our experimental results do not provide any new formation on the above problems, since in most cases the s-band is quite weak and thus structures are not easily seen. For the d-band region of Cu no experimental evidence for surface states is available from previous photoemission studies.[40,43] A calculation for the (001) surface predicts a maximum in the density of surface states around 4.6 eV below the Fermi level.[43] The question arises whether the peak at $\sim$5 eV BE which shows a broad resonance around 100 eV for Cu [001] corresponds to the calculated density of surface states. The spectra in Fig. 6, taken at $h\nu = 90$ eV, indicate that this is not the case. The solid line in Fig. 6a shows a spectrum taken at a normal take-off angle ($\alpha = 90°$) from a (001) face. The dashed line in Fig. 6b corresponds to a take-off angle of $\alpha = 35°$ from a (001) face (i.e. the [111] direction on the (001) face). Since the surface contribution

to the PED's is enhanced at low take-off angles,[44] a peak associated with the density of surface states should be increased at $\alpha = 35°$ relative to $\alpha = 90°$. However, the opposite is observed in Fig. 6, thus indicating that the peak at ~5 eV BE arises from bulk or bulk-like bands. It appears that, for Cu, the strong overlap of the bulk density of states with the density of surface states precludes one from gaining detailed information on the latter from these data.

Besides photoemission from surface states there has been considerable theoretical interest recently in studying the modification of bulk states near the surface.[45] The most interesting result of such calculations is the prediction of a narrowing of the d-band density of states near the surface.[45] In a simple physical picture such a behavior is expected because the reason for broadening atomic levels into solid-state bands is partly removed at the surface. We believe that we have observed this effect experimentally. As shown in Fig. 6 the experimental PED's along <u>both</u> the [001] and [111] directions become narrower when the take-off angle is changed from 90° to 35°. The above change in angle corresponds to a decrease in effective escape depth normal to the surface by a factor of 2. Thus in the low take-off angle ($\alpha = 35°$) case the surface derived contribution to the spectrum is considerably enhanced. The fact that the escape depth is already short at $h\nu = 90$ eV[11,36] makes us believe that we are largely sampling the outermost layer of the crystal in the low take-off angle case. The narrowing of the d-band width is accompanied by an increase of the central peak (~3.7 eV BE) which coincides with the center of gravity of the d-band. This is expected because of increased atomic

type behavior at the surface.

B. Au

The photon energy dependence of photoemission from polycrystalline Au was studied by Freeouf et al.[46] in the range 15 eV $\leq h\nu \leq$ 90 eV. Above $h\nu \approx 40$ eV the spectral features in the observed PED's did not change significantly. This was discussed by Feibelman and Eastman[26] in terms of momentum broadening in the final state. Measurements by Lindau et al.[10] up to 200 eV revealed dramatic changes in the shape of the 5d valence band in the range above 100 eV. For example, the intensity ratio of the low ($\sim$3.5 eV BE) and high ($\sim$6.5 eV BE) peak decreased from a value of 1.5 at $h\nu$ = 100 eV to 1.0 at $h\nu$ = 120 eV. Lindau et al. discussed several possible explanations for the observed modulation effects and favored an explanation in terms of an atomic-type cross-section effect. In particular, they associated the two main VB peaks with the spin-orbit-split components $5d_{5/2}$ and $5d_{3/2}$ and argued that the respective cross-sections may vary differently with photon energy. We can exclude this explanation on the basis of our experimental results.[47] An atomic type cross-section effect should also be seen in angle-resolved photoemission, i.e. in the range 100 eV $\leq h\nu \leq$ 120 eV for both Au [001] and Au [111]. Inspection of Fig. 7 or Fig. 8 reveals that this is not the case for Au [001]. The above argument also excludes an atomic cross-section effect of the Cooper-Fano type[48] as being responsible for the observed modulation effect in Au. This is independently confirmed by the photon energy dependence of the total Au 5d-band intensity (which is in good approximation proportional to the 5d cross-section) shown in Fig. 9. In

contrast to the case of the 4d intensity in Ag,[12,49] which exhibits a pronounced Cooper-minimum (cp. Fig. 9), the variation of the Au 5d intensity is not strong enough to significantly influence the shape of the valence band. We note that the PED's for Au [111] show a change in peak amplitudes for 100 eV $\leq h\nu \leq$ 120 eV (cp. Figs. 7 and 8) which goes in the same direction as those observed by Lindau et al.[10] In fact, the low BE peak decreases by a factor of 1.6 from $h\nu$ = 100 eV to $h\nu$ = 120 eV. Similar to the ARP results obtained for Cu, band structure induced cross section effects (i.e. final state plus matrix element effects) are thus found to be important for angle resolved photoemission from Au above 100 eV. In the light of the present results preferrential orientation of the crystallites in evaporated Au films may cause modulation effects similar to those observed in reference 10. In fact, such effects were observed for evaporated Au samples by Koyama and Hughey[50] at lower photon energies.

At the highest photon energies the Au spectra for photoemission along the [001] and [111] directions have not converged to the XPS limit[3] (also compare Fig. 12). Direct transition effects still appear to be important. In contrast to the case of Cu, the PED's for Au [001] and Au [111] do not reveal any resemblence to the e_g and t_{2g} projections of the initial density of states (cp. Fig. 12) in the surface sensitive energy range around 90 eV.[36] This finding does not necessarily lead to the conclusion that the resemblence of the ARP spectra for Cu with the initial state projections is accidental in this energy range, but rather may imply that the case of Au is more complicated. Complications may arise from interference effects in the final state due to the

photoelectron-ion core interaction[39] and the larger spin-orbit coupling.

VI. CONCLUSIONS

In this paper we have shown that, in contrast to angle integrated photoemission measurements, ARP spectra have not converged to the XPS limit at the highest photon energies studied. This is attributed to the importance of direct transitions which restrict transitions to occur in only part of the Brillouin Zone. In the case of Cu the PED's taken around $h\nu$ = 85 eV along the [001] and [111] directions are found to resemble the e_g and t_{2g} projections of the initial 3d density of states, similar to the spectra taken at XPS energies.[3,35] Momentum broadening in the final state due to a short inelastic mean free path in this energy region is discussed as a possible reason for such behavior. At $h\nu$ = 90 eV a narrowing of the Cu PED's taken along equivalent symmetry directions is observed when the take-off angle is lowered from 90° to 35°. This is attributed to a preferrential sampling of the surface local density of states by using an appropriate photon energy and a low take-off angle. For Au, the cross section of the 5d valence band has been measured as a function of photon energy. This is the first measurement of this kind for a 5d initial-state wavefunction. Furthermore we have presented new information on the modulation effects of the 5d valence band peaks above $h\nu$ = 100 eV, which were previously reported for photoemission from polycrystalline Au.[10] We hope that the present experimental results will stimulate a detailed theoretical calculation, which may cast more light on the complex role of cross-section versus surface effects in the transition region between UPS and XPS.

ACKNOWLEDGEMENTS

We would like to thank Mrs. Winifred Heppler for preparing the Cu single crystals, Professor Gabor Somorjai for supplying the Au single crystals, and R. Gaxiola and the SSRP staff for their cooperation during the course of the experiments.

One of us (J.S.) would like to acknowledge the Deutsche Forschungsgemeinschaft for granting a stipend.

FOOTNOTES AND REFERENCES

*This work was performed at the Stanford Synchrotron Radiation Project, which is supported by the National Science Foundation Grant No. DMR 73-07692 A02, in cooperation with the Stanford Linear Accelerator Center. The electron analyzer was purchased by funds obtained from NSF Grant No. GH-40132. This work was done with support from the U.S. Energy Research and Development Administration. Any conclusions or opinions expressed in this report represent soley those of the authors and not necessarily those of The Regents of the University of California, the Lawrence Berkeley Laboratory or the U.S. Energy Research and Development Administration.

1. For a recent review see B. Feuerbacher and R. F. Willis, J. Phys. C 9, 169 (1976).
2. R. J. Baird, L. F. Wagner, and C. S. Fadley in Faraday Discussion on Electron Spectroscopy of Solids and Surfaces, Vancouver, British Columbia, July, 1975 (to be published), and private communication.
3. F. R. McFeely, J. Stöhr, G. Apai, P. S. Wehner, and D. A. Shirley, submitted for publication.
4. See for example reference 1, p. 182 - 185.
5. For a recent review see: D. E. Eastman in Vacuum Ultraviolet Radiation Physics, Edit. E. E. Koch, R. Haensel, and C. Kunz, (Pergamon, Vieweg 1974), p. 417.
6. H. Winick in reference 5, p. 776.

7. Synchrotron radiation experiments at SSRP are usually carried out in a parasitic mode on high-energy physics experiments. Typical electron beam currents are ∿15 mA.

8. I. Lindau and W. E. Spicer, J. Electron Spectroscopy 3, 409 (1974), C. R. Brundle, Surface Science 48, 99 (1975).

9. C. Caroli, D. Lederer-Rozenblatt, B. Roulet, and D. Saint-James, Phys. Rev. B8, 4552 (1973).

10. I. Lindau, P. Pianetta, K. Y. Yu, and W. E. Spicer, Phys. Rev. B13, 492 (1976).

11. J. Stöhr, F. R. McFeely, G. Apai, P. S. Wehner, and D. A. Shirley, (Results on polycrystalline Cu for 50 eV $\leq \hbar\omega \leq$ 175 eV submitted for publication).

12. P. S. Wehner, J. Stöhr, G. Apai, F. R. McFeely, R. S. Williams, and D. A. Shirley (Results on polycrystalline Ag for 40 eV $\leq \hbar\omega \leq$ 250 eV submitted for publication).

13. F. C. Brown, R. Z. Bachrach, S. B. M. Hagström, N. Lien, and C. H. Pruett in reference 5, p. 785.

14. P. W. Palmberg, J. Electron Spectrosc. 5, 691 (1974).

15. H. Niehus and E. Bauer, Rev. Sci. Instrum. 46, 1275 (1975). It should be noted that the CMA used in our study (Physical Electronics) does not accept electrons equally into its 360° acceptance cone. There are posts in four (1.5, 4.5, 7.5, and 10.5 o'clock) positions inside the analyzer which block the electrons along the respective trajectories. This fact has to be considered when rotating the slit for angle resolved studies as proposed in the above reference. In our case the slit was fixed in the 3 o'clock position and hence

the posts had no effect on our measurements.

16. The value $\Delta\alpha = 6°$ for the acceptance angle of the CMA quoted in reference 14 (footnote Fig. 1) is incorrect and should read $\Delta\alpha = 12°$ or $\alpha = (42.3 \pm 6)°$.

17. These measurements were performed on the spin-orbit split $4d_{3/2}$ and $4d_{5/2}$ doublet of Indium.

18. Assuming a constant band pass of 0.1 Å (reference 13) the resolution of the monochromator is given by $\Delta E = 8 \times 10^{-6} (h\nu)^2$ where both ΔE and $h\nu$ are in units of eV. However, at higher photon energies ($h\nu > 200$ eV) imperfections in the gratings and in the reflecting mirror surfaces appeared to increase the resolution over the above value.

19. L. Ilver and P. O. Nilsson, Solid State Comm. 18, 677 (1976).

20. P. O. Nilsson and L. Ilver, Solid State Comm. 17, 667 (1975).

21. J. F. Janak, A. R. Williams, and V. L. Moruzzi, Phys. Rev. B11, 1522 (1975).

22. N. E. Christensen and B. O. Seraphin, Phys. Rev. B4, 3321 (1971).

23. We are aware of only one band structure calculation extending above 100 eV, namely for Aℓ by V. Hoffstein and D. S. Boudreaux, Phys. Rev. B2, 3013 (1970). Recently a high-energy band structure of Au extending up to ∿60 eV has been published by N. E. Christensen, Phys. Rev. B13, 2698 (1976).

24. Following G. D. Mahan, Phys. Rev. B2, 4334 (1970), the emission directions are often discussed in terms of "primary" and "secondary" cones.

25. See for example the review article by J. W. Gadzuk in Electronic Structure and Reactivity of Metal Surfaces, NATO Advanced Study

Institute Series (Plenum Press, N. Y. 1976).

26. P. J. Feibelman and D. E. Eastman, Phys. Rev. B10, 4932 (1974).

27. A. Liebsch, Phys. Rev. B13, 544 (1976).

28. J. B. Pendry, Low Energy Electron Diffraction, (Academic, New York, 1974); C. B. Duke in Dynamic Aspects of Surface Physics, edited by F. O. Goodman (Editrice Compositori, Bologna, 1974), p. 99; D. W. Jepsen, P. M. Marcus, and F. Jona, Phys. Rev. B5, 3933 (1972).

29. R. O. Jones and J. A. Strozier, Phys. Rev. Lett. 22, 1186 (1969); C. B. Duke and C. W. Tucker, Phys. Rev. Lett. 23, 1163 (1969).

30. R. F. Willis and B. Feuerbacher, Surface Science 53, 144 (1975).

31. In addition to matrix element effects which arise from the details of the band structure, atomic type matrix element effects may be observed if the initial state wavefunction has a radial node (ref. 12).

32. In order to estimate the most important $\vec{G}$ vector at a given photon energy one may use the free electron relation $h\nu$ (eV) = $(12.26/a)^2 (G_x^2 + G_y^2 + G_z^2)$ where a is the lattice constant in Angstrom, and $|\vec{G}|$ is in units of $2\pi/a$.

33. N. V. Smith, Phys. Rev. B3, 1862 (1971).

34. L. Hodges, H. Ehrenreich, and N. D. Lang, Phys. Rev. 152, 505 (1966).

35. These results will be published by us separately.

36. I. Lindau, P. Pianetta, K. Y. Yu, and W. E. Spicer, J. Electron Spectroscopy 8, XXX (1976).

37. These states are allowed by the momentum conservation selection rule. Whether they actually contribute depends on satisfaction of the energy conservation selection rule.

38. S. T. Manson, Phys. Rev. 182, 97 (1969).

39. For p waves the phase shifts at threshold are 6.26 (Cu) and 12.40 (Au). For f waves the values are 0 (Cu) and 3.17 (Au) (compare reference 38).

40. Reference 1, page 203 ff.

41. P. O. Gartland and B. J. Slagsvold, Phys. Rev. B12, 4047 (1975).

42. K. L. Kliewer, Phys. Rev. Lett. 33, 900 (1974).

43. S. J. Gurman, Surface Science 55, 93 (1976).

44. W. A. Fraser, J. V. Florio, W. N. Delgass, and W. D. Robertson, Surface Science 36, 661 (1973); C. S. Fadley, R. Baird, W. Siekhaus, T. Novakov, and S. A. L. Bergstrom, J. Electron Spectr. 5, 725 (1975).

45. For a review see reference 1, p. 171 - 174, and p. 203 - 211.

46. J. Freeouf, M. Erbudak, and D. E. Eastman, Solid State Comm. 13, 771 (1973).

47. Furthermore, we believe that the two Au 5d valence band peaks cannot be discussed in terms of the two spin-orbit-split components $5d_{5/2}$ and $5d_{3/2}$ since solid-state effects are dominant.

48. Such an effect has been observed for polycrystalline Ag. Compare reference 12 and references therein.

49. We have measured some preliminary angle resolved PED's for Ag [001] and Ag [111] up to $h\nu$ = 130 eV. These spectra also reveal the atomic cross-section effect discussed in reference 12.

50. R. Y. Koyama and L. R. Hughey, Phys. Rev. Lett. 29, 1518 (1972).

Table I. EXPERIMENTAL GEOMETRY FOR PHOTOEMISSION FROM SINGLE CRYSTALS OF Cu AND Au

	Cu [001][b]	Cu [111][b]	Au [001][b]	Au [111][b]
$\vec{E}$ VECTOR[a]	$\Theta = 27.5°$ $\phi = 45°$	$\Theta = 27.5°$ $\phi = 45°$	$\Theta = 27.5°$ $\phi = 60.0°$	$\Theta = 30.0°$ $\phi = 26.5°$
DETECTOR[a]	$\Theta = 0°$ (along z axis)	$\Theta = 54.5°$ $\phi = 45°$	$\Theta = 0°$ (along z axis)	$\Theta = 54.5°$ $\phi = 45°$

a) All values have been rounded to the nearest 0.5°.

b) Electrons were taken off normal to the (001) and (111) crystal faces, respectively.

FIGURE CAPTIONS

Fig. 1. Experimental geometry for angle resolved photoemission studies of Cu and Au single crystals. A cylindrical mirror analyzer (CMA) is modified by means of a slit aperture (shield) to allow measurements with an angular resolution of $\sim\pm 6°$.

Fig. 2. Experimental orientation of the x-ray beam, $\vec{E}$ vector and detector relative to the fourfold cubic crystalline axes x,y,z. The polar (Θ) and azimuthal (ϕ) angles define the orientation of the $\vec{E}$ vector in the coordinate system x,y,z. The crystal could be rotated about a vertical axis. The x-ray beam, $\vec{E}$ vector and detector positions were fixed in a laboratory frame of reference and lay in the horizontal plane.

Fig. 3. Photoemission energy distributions from Cu single crystals in the range 32 eV $\leq h\nu \leq$ 200 eV. The Cu [001] and Cu [111] spectra were obtained by taking electrons off normal to the (001) and (111) single crystal faces (compare Figs. 1 and 2 and Table I). The spectra are also shown enlarged around the Fermi energy.

Fig. 4. Comparison of photoemission spectra taken along the Cu [001] and [111] directions (dashed and solid lines, respectively) for various photon energies. The experimental geometry was the same as for Fig. 3.

Fig. 5. Photoemission from a Cu (001) face at $h\nu$ = 120 eV into the normal [001] direction (Θ = 27.5°) and into a direction 4° off the normal take-off direction (Θ = 23.5°). Θ is defined

in Fig. 2a. In both cases $\phi = 45°$. The dashed spectrum corresponds to a detector orientation of $\Theta_D = 4°$, $\phi_D = 225°$ in the frame x,y,z.

Fig. 6. a) Comparison of photoemission spectra of Cu taken for electrons propagating along a [001] direction normal to a (001) crystal face ($\alpha = 90°$) and at a take-off angle of $\alpha = 35°$ from a (111) crystal face. The solid line corresponds to $\Theta = 27.5°$ and $\phi = 45°$ in Fig. 2a, the dashed line to $\Theta = 27.5°$, $\phi = 225°$ in Fig. 2b.

b) Spectra taken along a Cu [111] direction normal to a (111) crystal face ($\alpha = 90°$) and at a take-off angle of $\alpha = 35°$ from a (001) crystal face. The solid line corresponds to $\Theta = 27.5°$, $\phi = 45°$ in Fig. 2b, the dashed line to $\Theta = 82.5°$ and $\phi = 45°$ in Fig. 2a.

Fig. 7. Photoemission spectra from Au single crystals in the range $32\ eV \leq h\nu \leq 130\ eV$. The Au [001] and Au [111] spectra correspond to photoelectron propagation normal to the (001) and (111) single crystal faces (cp. Fig. 1 and 2 and Table I).

Fig. 8. Comparison of photoemission energy distributions along the [001] and [111] direction of Au (dashed and solid lines) in the range $32\ eV \leq h\nu \leq 120\ eV$. The spectra were taken from Fig. 7.

Fig. 9. Relative intensity of the 4d valence band of Ag (reference 12) and the 5d valence band of Au as a function of photon energy. The Ag and Au valence band intensities were normalized with respect to each other at $h\nu = 40\ eV$.

Fig. 10. a) (010) projection of the three dimensional Brillouin Zone of a fcc lattice. The $\vec{k}$ axes are those of the infinite three-dimensional crystal.

b) Photoemission along the [001] direction assuming an angular resolution of ±6° (dashed area). The dashed area within the various zones indicates the fraction of initial states sampled in the first Brillouin Zone if the final state contains the respective $\vec{G}$ vector.

Fig. 11. Total valence band (VB) density of states and the t_{2g} and e_g projections for Cu 3d calculated in a tight binding interpolation scheme as discussed in the text. The density of states histograms were convoluted with a Gaussian of FWHM = 0.5 eV.

Fig. 12. Total valence bands (VB) density of states and the t_{2g} and e_g projections for the 5d band in Au. Calculations were carried out as for Fig. 11, with a spin orbit coupling constant of 0.048 Ry included. A Gaussian of FWHM = 0.8 eV was used to convolute the density of states histograms.

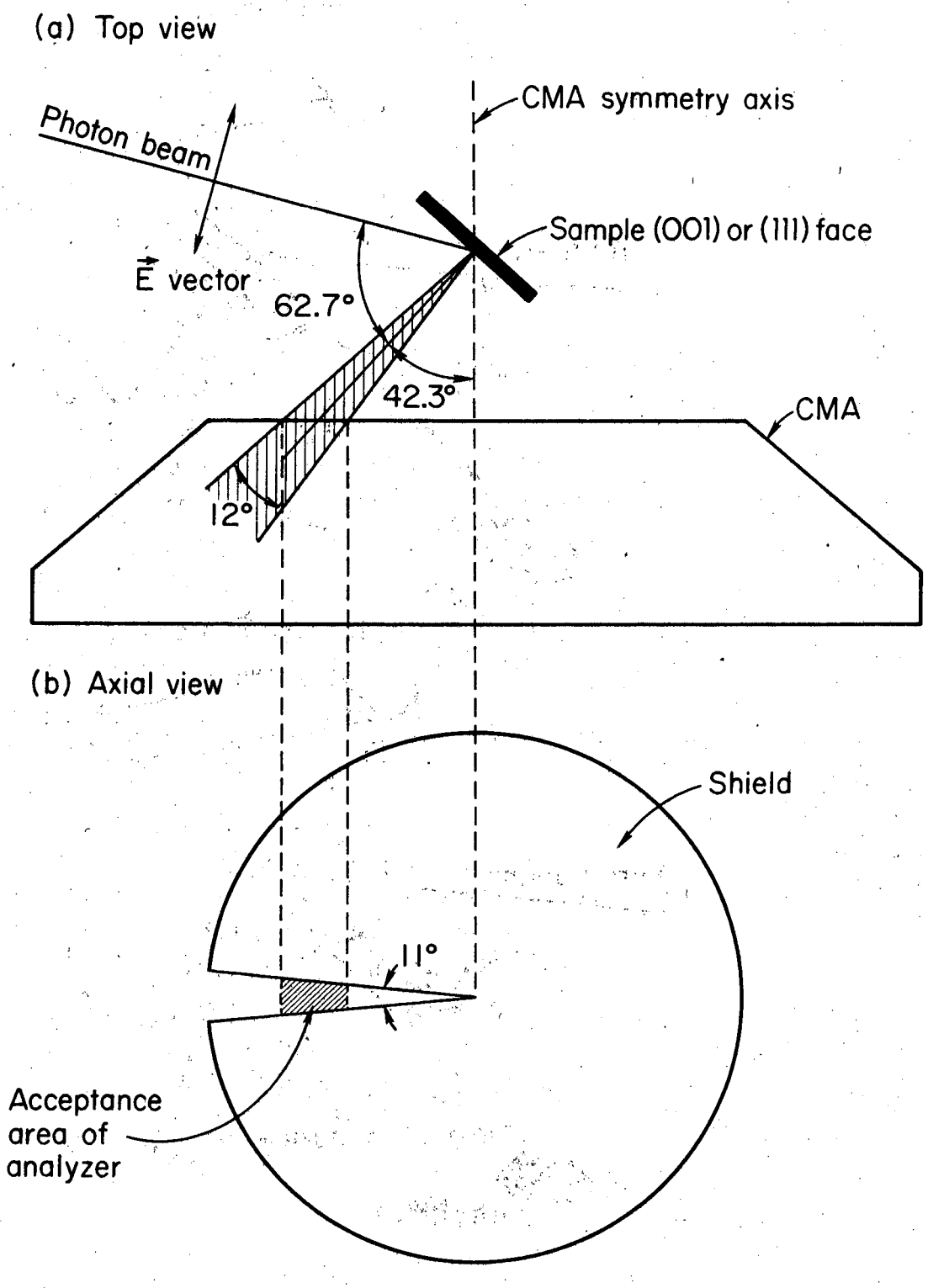

Fig. 1

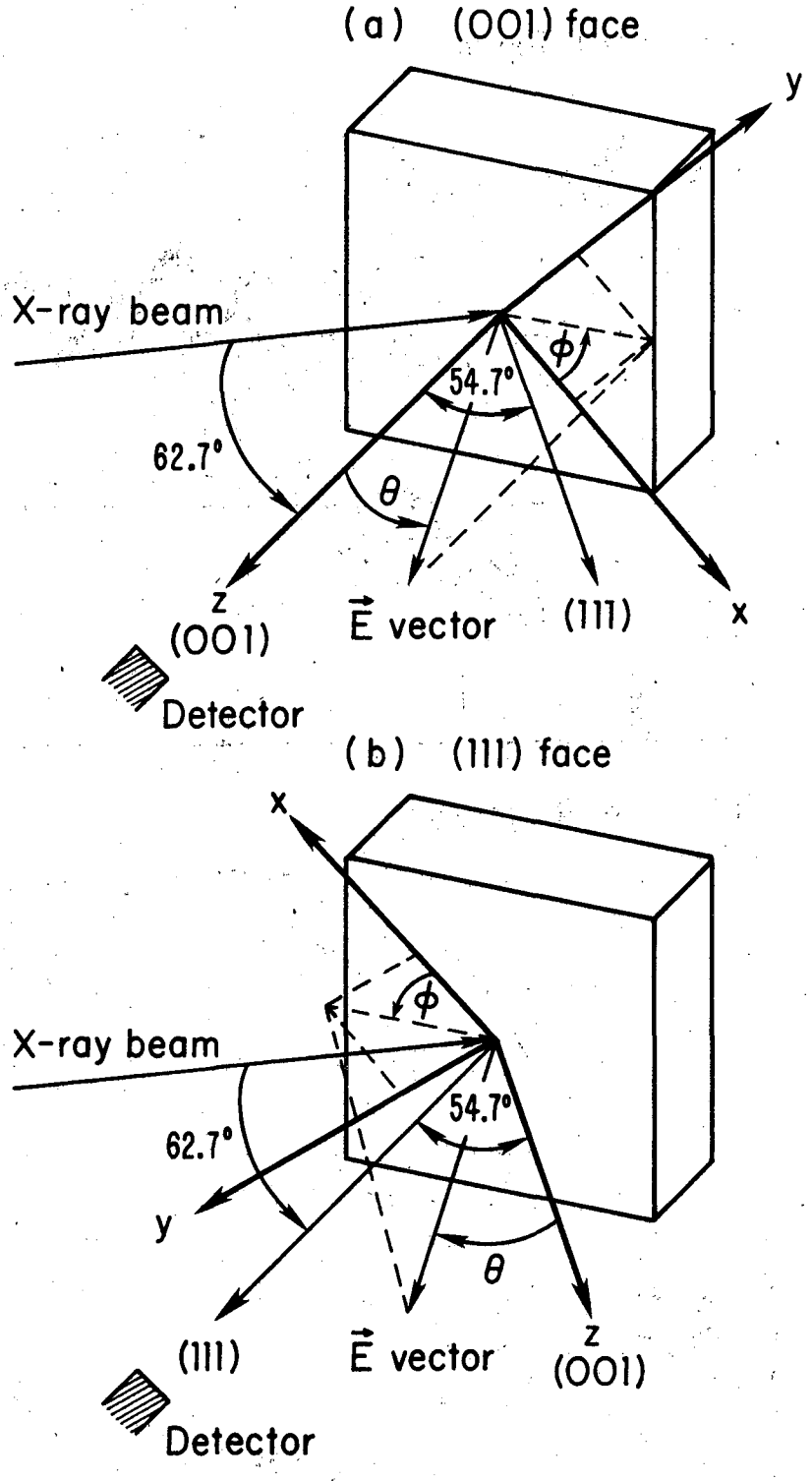

XBL 763-2526

Fig. 2

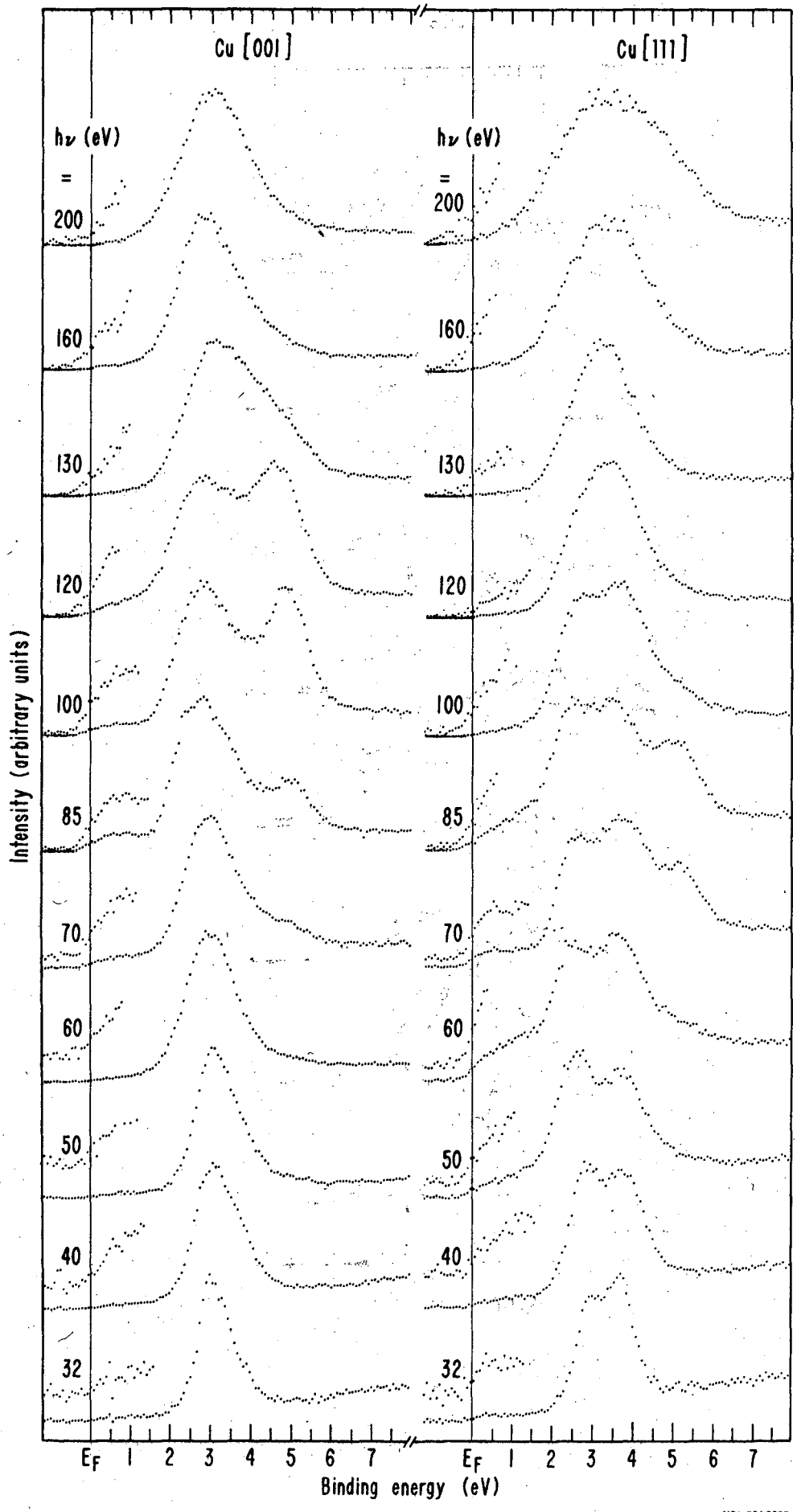
Cu [001]
Cu [111]
hν (eV)
=
200
160
130
120
100
85
70
60
50
40
32
Intensity (arbitrary units)
E_F 1 2 3 4 5 6 7
Binding energy (eV)
XBL 764-2807

Fig. 3

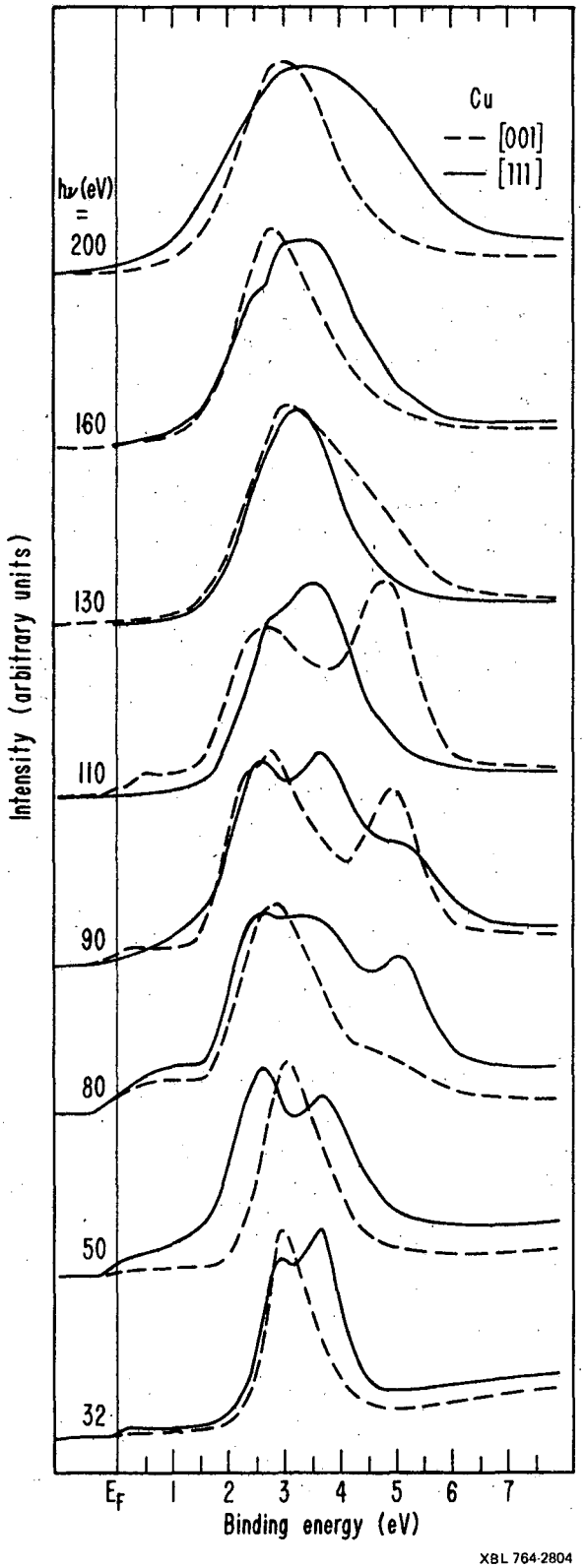
Cu
[001]
[111]
hν(eV)
=
200
160
130
110
90
80
50
32
Intensity (arbitrary units)
E_F
1
2
3
4
5
6
7
Binding energy (eV)
XBL 764-2804

Fig. 4

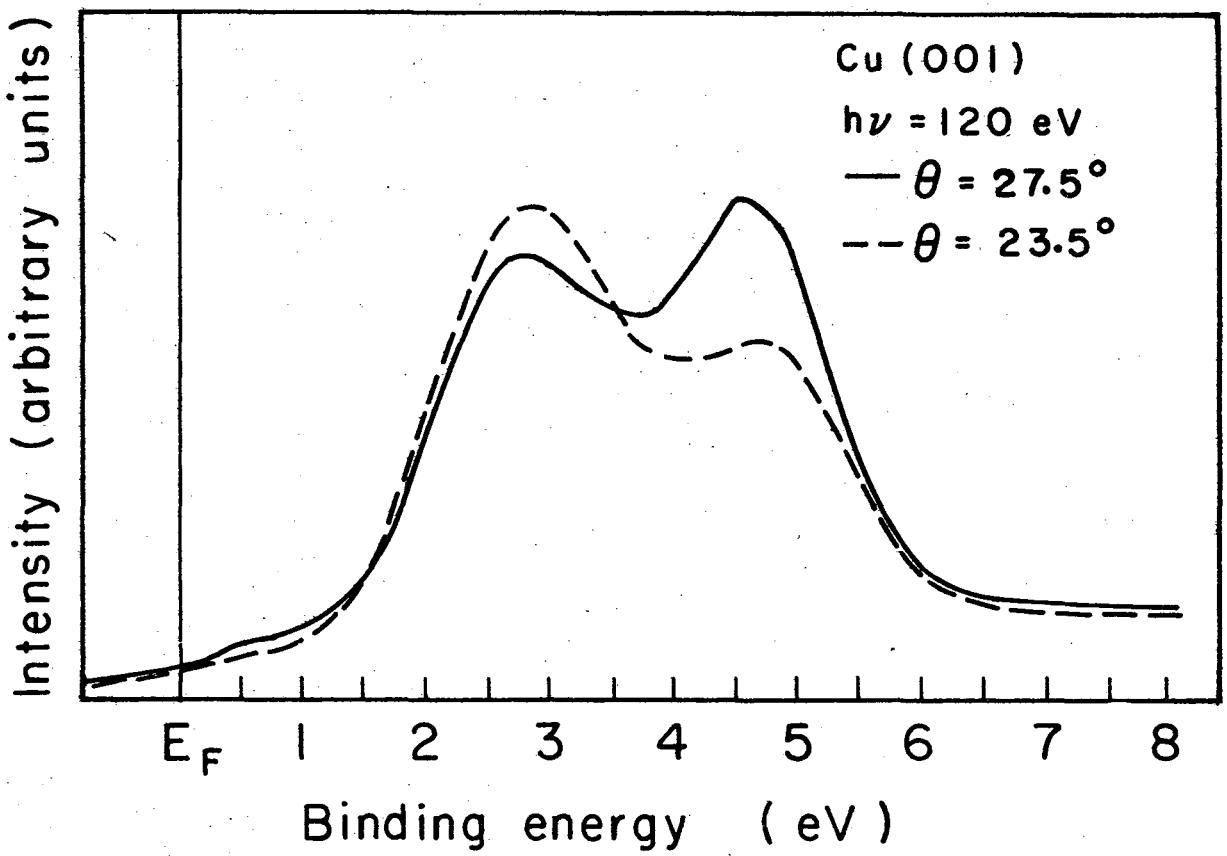

XBL 764-2765

Fig. 5

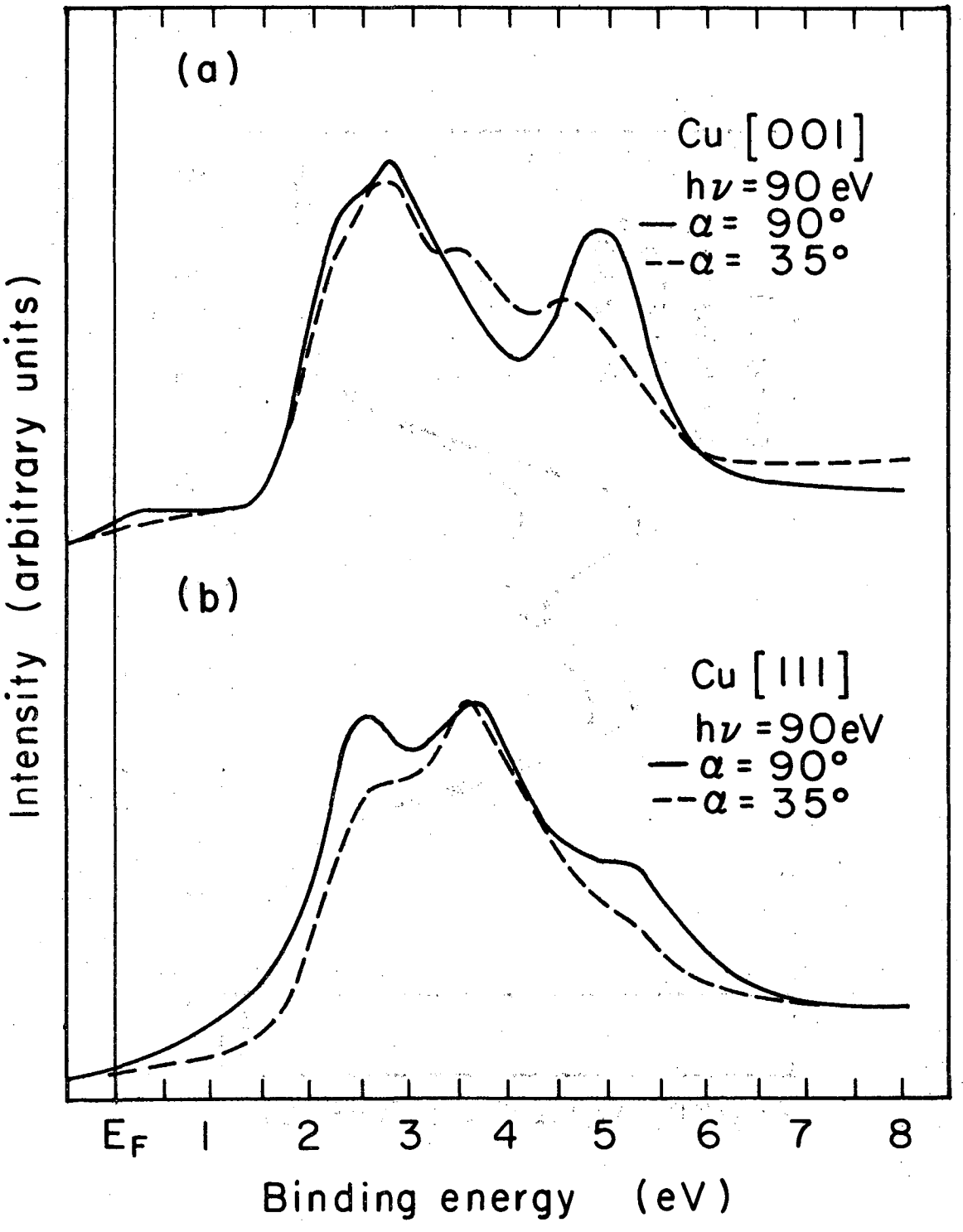

XBL 764-2764A

Fig. 6

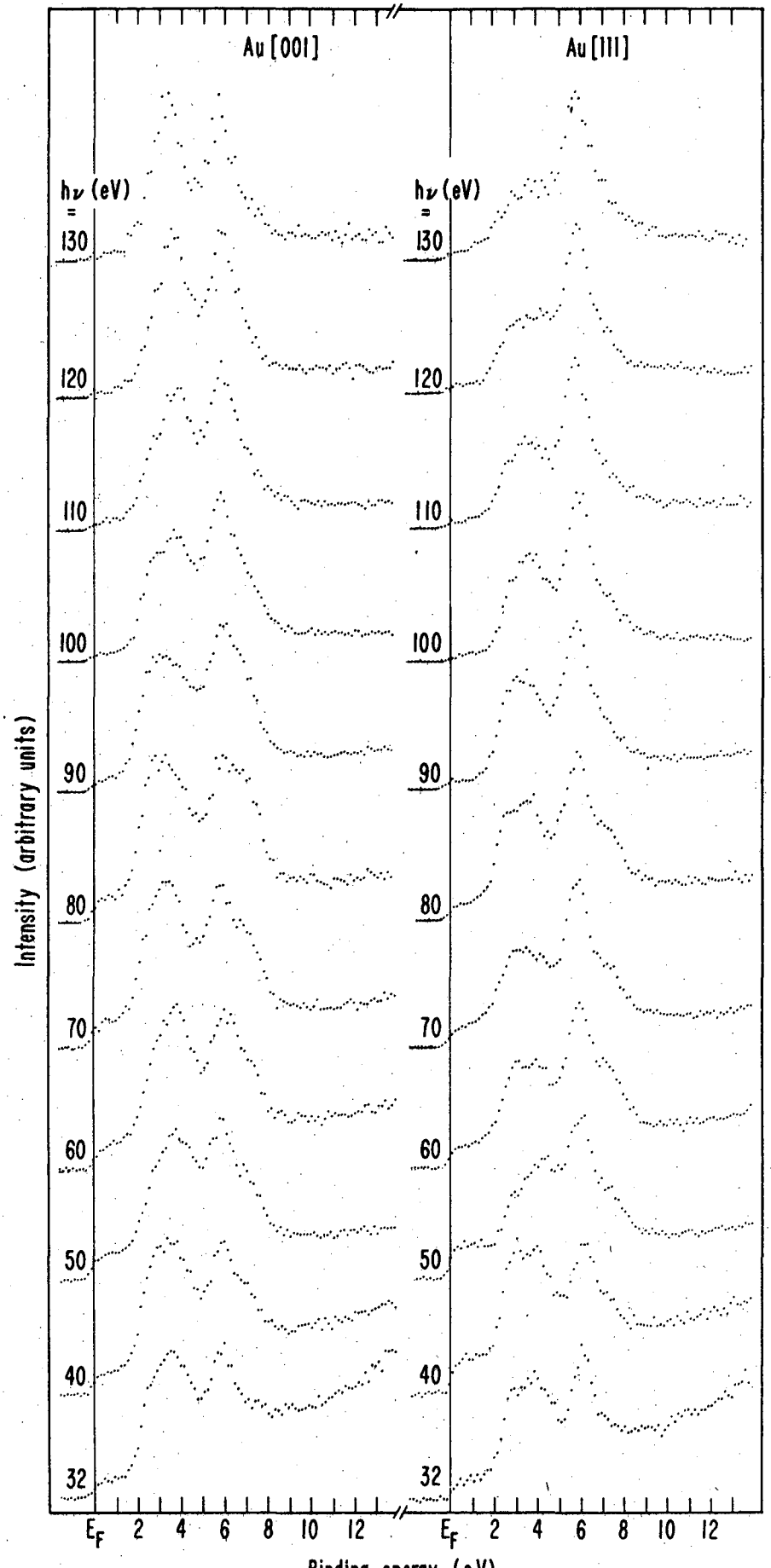

Fig. 7

XBL 764-2806

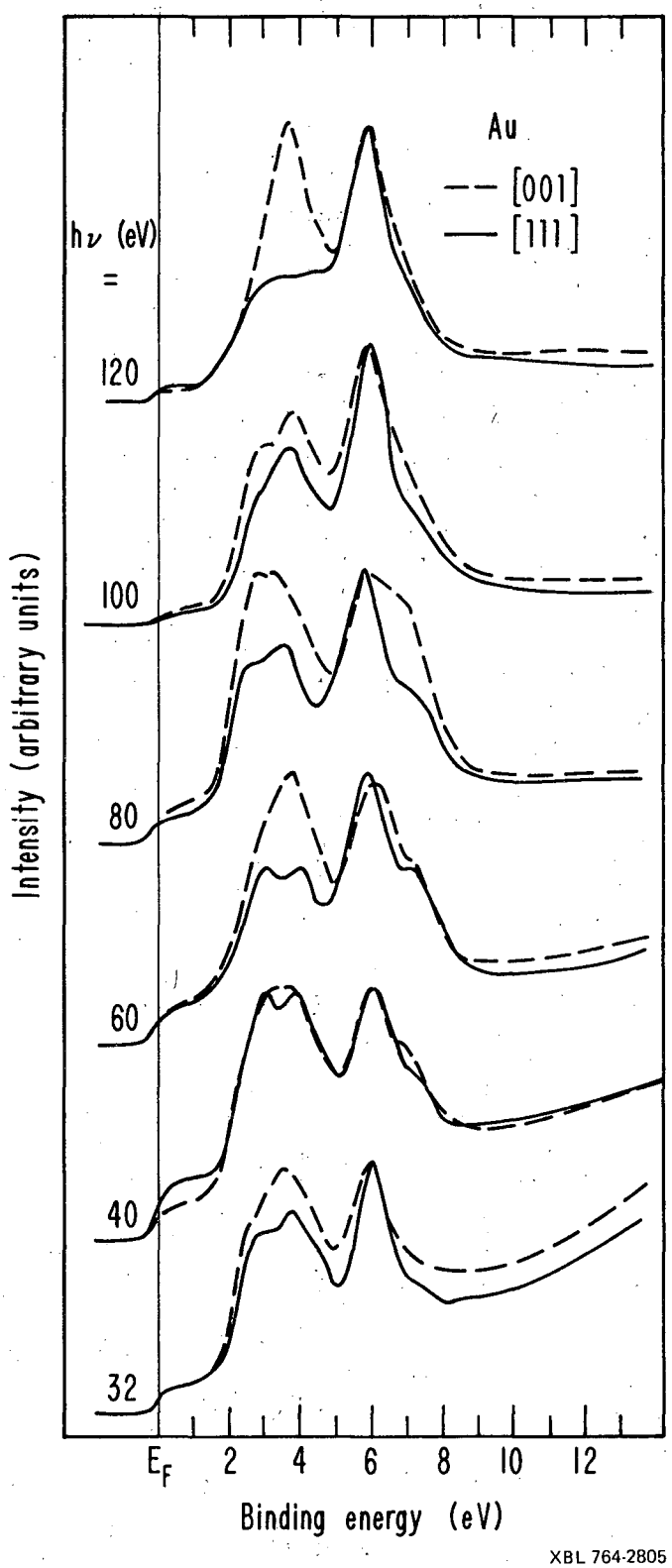

XBL 764-2805

Fig. 8

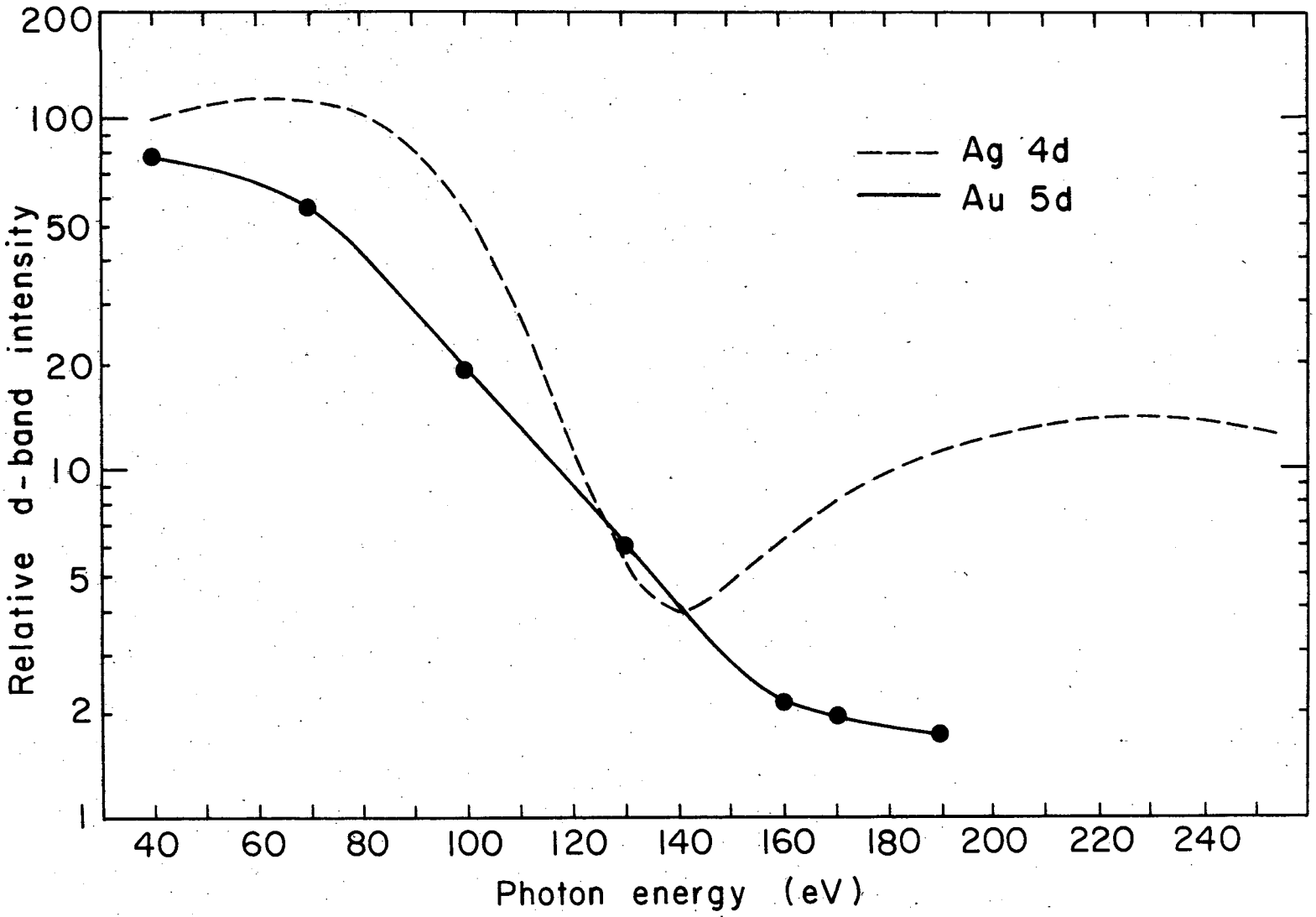

XBL764-2763

Fig. 9

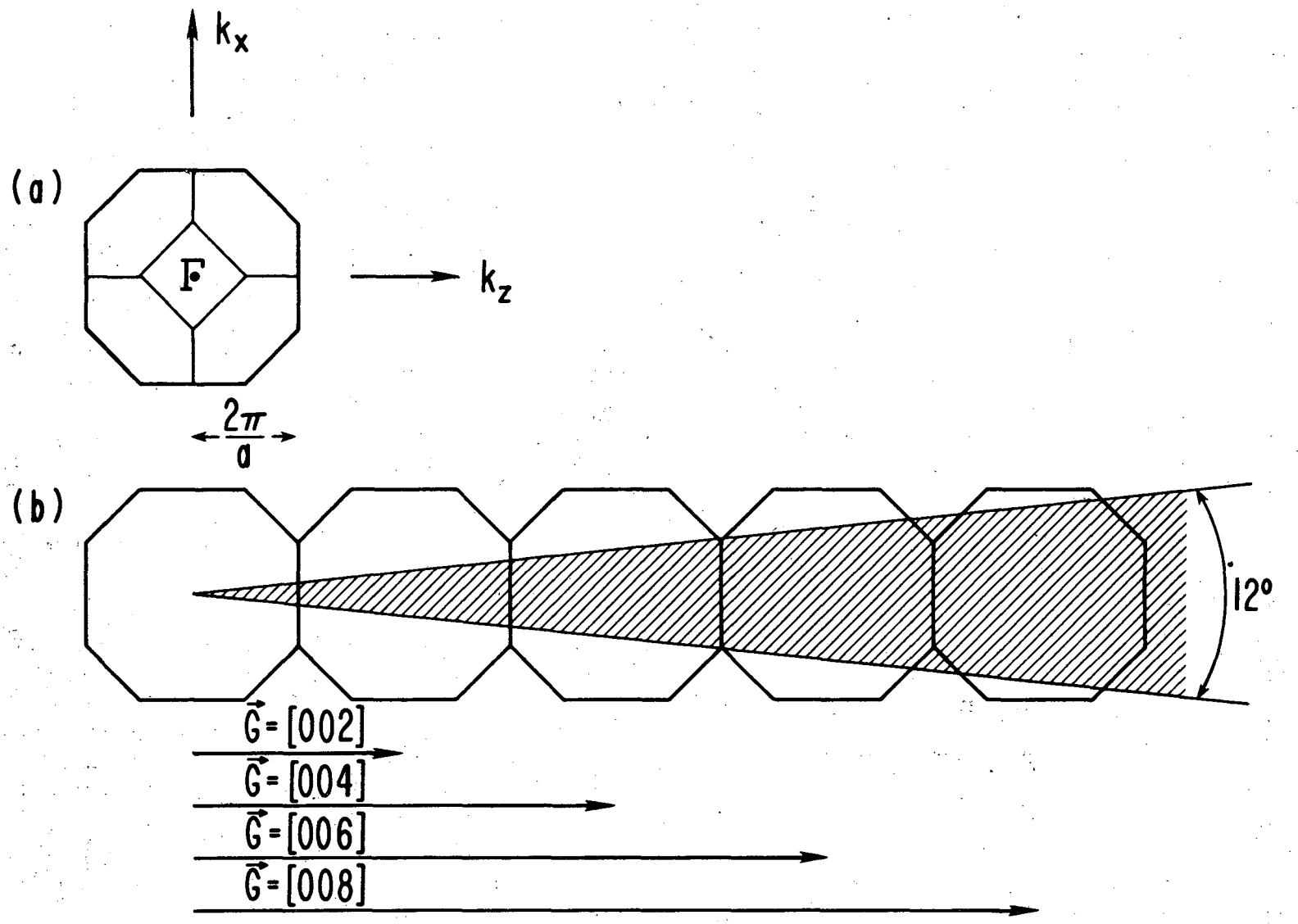

XBL 765-1951

Fig. 10

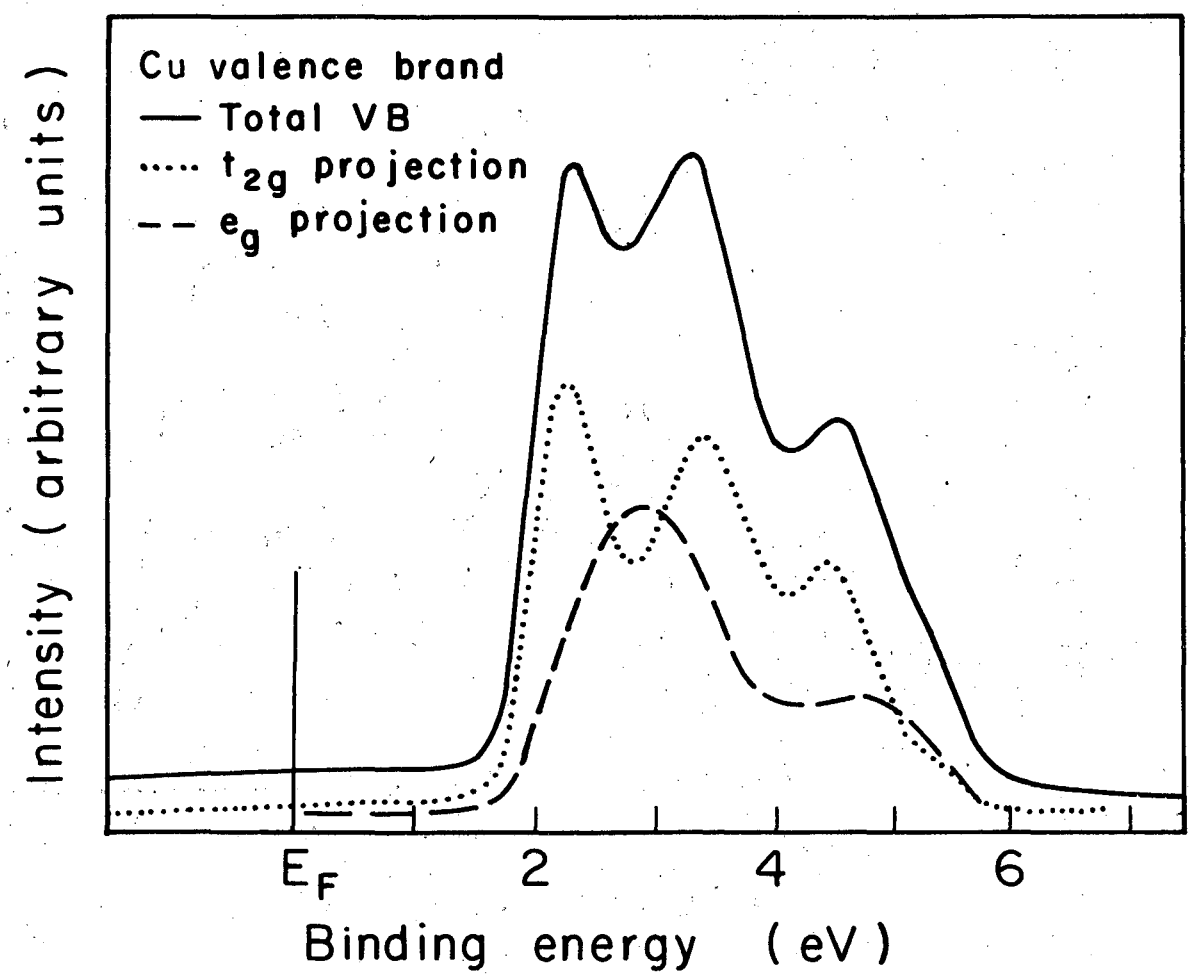

XBL 764-2735

Fig. 11

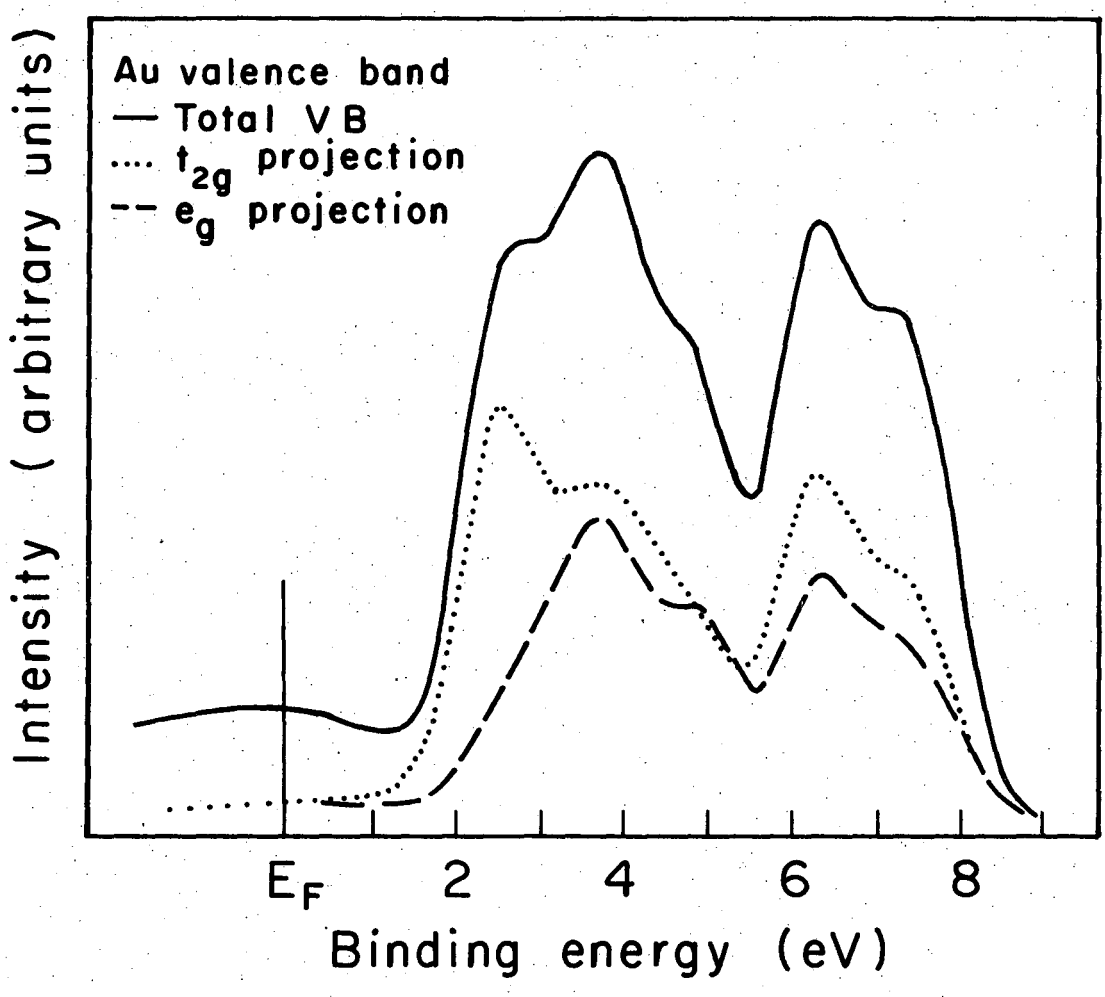

XBL 764-2736

Fig. 12

TECHNICAL INFORMATION DIVISION
LAWRENCE BERKELEY LABORATORY
UNIVERSITY OF CALIFORNIA
BERKELEY, CALIFORNIA 94720